Mechanics of Advanced Composite Structures 10 (2023) 43 – 52

Semnan University

Mechanics of Advanced Composite Structures

journal homepage: http://MACS.journals.semnan.ac.ir

Maximization of Fundamental Frequency of Composite Stiffened Hypar Shell with Cutout by Taguchi Method

P.B. Chaudhuri [a], A. Mitra [b], S. Sahoo [a]*

[a] *Department of Civil Engineering, Heritage Institute of Technology, Kolkata, 700107, India*
[b] *Department of Mechanical Engineering, Jadavpur University, Kolkata, 700032, India*

KEYWORDS

Laminated hypar shells;
Stiffener;
Cutout;
Fundamental frequency;
Optimization;
Taguchi method.

ABSTRACT

Composite shells find extensive application in modern civil, aerospace, and marine structures. In order to avoid resonance, such load-carrying shells need to be optimized from a frequency perspective. Composite shell structures often include cutouts for different functional requirements. Obtaining the best combination of design variables like degree of orthotropy, ply orientation, shallowness of the shell, and eccentricity of cutout of laminated shells leads to a problem of combinatorial optimization. This article attempts a numerical study of the free vibration response of composite stiffened hypar shells with cutout using finite element procedure and optimization of different parametric combinations based on the Taguchi approach. Numerical investigations are carried out following the L27 Taguchi design with four design factors, viz., fiber orientation, width/thickness factor of shell, degree of orthotropy, and position of the cutout for different edge constraints. For different shell boundaries considered here, the width/thickness factor emerges as the most influencing factor followed by a degree of orthotropy. The optimum parametric combination for the maximum fundamental frequency of cutout borne stiffened hypar shell is obtained from the analysis.

1. Introduction

Competitive demands like lightweight, reduced cost, environment-safe, sustainability, dimensional stability, etc. have led to the development of laminated composites. Composites find extensive use in different structural applications of mechanical, aerospace, and civil engineering. Fibre-reinforced composites help in the reduction of noise transmission and vibration of structures due to high internal damping. Accordingly, laminated composite is a material of choice for structural designers. Among various shell forms, aesthetically appealing skewed hypar shells are widely used in roof structures demanding large column-free areas. Examples include hangers, auditoriums, exhibition halls, railway stations, etc. Shell boundaries are quite often kept free to meet practical requirements. Thin-walled shell structures do perform better when provided with stiffeners, particularly when cutouts are present on the shell surface. Cutouts become a necessity in structural roofs for several requirements like the passage of light, accessibility to different parts, venting, alteration of resonant frequency, etc. The vibration frequencies of laminated panels depend on laminations, edge conditions, shell dimensions (thickness, length), and cutout (size and position) [1-3]. Therefore, for cutout borne stiffened hypar shells with various material systems and geometric shapes, obtaining an appropriate combination of lamination angle, thickness, cutout position, and end conditions for maximization of the fundamental frequency becomes an interesting problem. This is more so because fundamental frequency needs to be higher to skip any resonance effect occurring from ground vibrations and other natural disturbances. However, there has not been much activity in this respect perhaps due to the complexities involving so many shell parameters and complicated algorithm flow as well.

Design of stacking sequence for optimization of vibration frequency of laminated structures is

* Corresponding author. Tel.: +91-3324160358
E-mail address: sarmila.sahoo@gmail.com; sarmila.sahoo@heritageit.edu

DOI: 10.22075/macs.2022.27206.1405
Received 2022-05-23; Received in revised form 2022-09-22; Accepted 2022-10-22.

a common approach [4-6]. Discrete material optimization [7] using a finite element approach has also been attempted for the optimization of fiber angle and material. A genetic algorithm is employed for the optimization of composite structures with respect to vibration and buckling [8-10]. A modified feasible direction technique was utilized [11, 12] to maximize the fundamental frequency for varying thickness ratios and aspect ratios of shells. Other modern advanced heuristic algorithms [13-21] were also utilized for the stacking sequence design of composites. However, features of most heuristic algorithms are random in the search process. Accordingly, local optimum or pre-convergence may occur if initial parameters are unsuitable. Reliable optimization results depend only on the designers' experience. Also, the computational cost of heuristic algorithms is relatively high. Thus, researchers are in the search of alternative ways of optimization [22]. Shahgholian-Ghahfarokhi and Rahimi [23] recently used the Taguchi approach [24] to consider a sensitivity study of the vibration of composite sandwich cylindrical shells having grid cores. The dynamic behavior of plates and shells made of different types of materials has been analyzed [25-27]. Galerkin method coupled with higher order shear deformation theory has been used for analyzing the stability and vibration behavior of the such structure under different types of loadings [28-33].

Despite a good number of studies on the maximization of fundamental frequency by appropriate design of stacking sequence, extensive scrutiny of the literature reveals a paucity of reports on optimization of the fiber orientation, dimension, thickness, material orthotropy, and position of the cutout for different edge constraints leading to the maximum fundamental frequency of laminated shells.

This study of stiffened hypar shells considers the application of the Taguchi method [24] along with an efficient finite element formulation to determine the suitable combination of multi-parametric design optimization to yield the maximum frequency of cutout borne shell. Taguchi orthogonal design is applied with four design factors namely, fiber orientation, width-to-thickness, level of orthotropy of the composite, and position of the cutout as independent variables. Taguchi analysis is performed to obtain the suitable combination of factors that results in maximum fundamental frequency. A confirmation analysis verified the optimal parametric combination obtained from the Taguchi approach. Analysis of variance (ANOVA) was performed to get the significant design factors and the level of significance of their interactions.

2. Taguchi Method

Taguchi method [24, 34] employs orthogonal array (OA) based experiments that help in reducing the variance with the optimum combination of control factors. For achieving the same, it integrates the design of experiments (DOE) technique with the optimization of control factors. For performance analysis, traditional experimental designs use the average of characteristics while the Taguchi method is based on the effect of variation of the characteristics. In essence, the performance of the system becomes insensitive to the variation of noise factors. Standard OA helps to evaluate the ability of design parameters in controlling the variability of a particular characteristic by performing the least number of tests.

Thus, the Taguchi method considers the total design space using a reduced number of experiments to evaluate all of the design factors and interactions. The optimal setting of the design factors for maximizing the objective function is thus obtained. The factor trends and noise sensitivities are also obtained. The flowchart in Taguchi design is shown in Fig. 1.

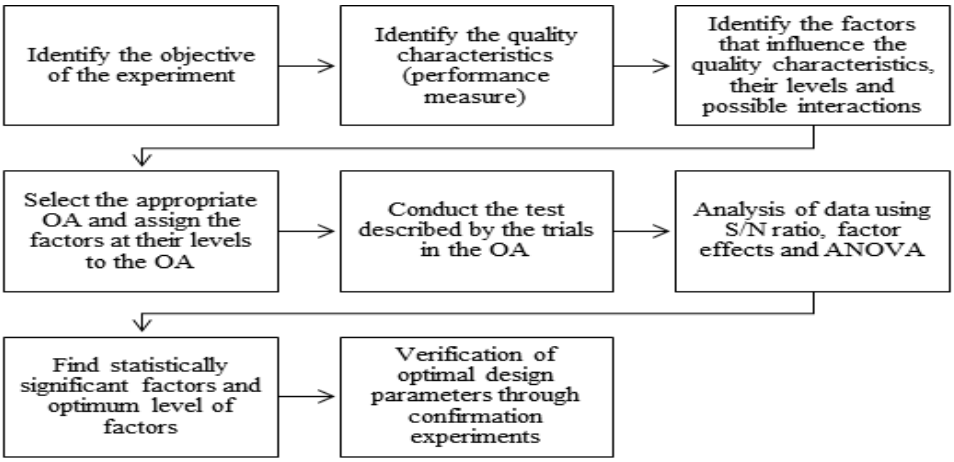

Fig. 1. Flow chart in Taguchi design

Taguchi optimization uses signal-to-noise (S/N) ratio as the objective function. The S/N ratio considers the mean (signal) as well as the variability (noise). It depends on the type of design. Three types of S/N ratios are defined: Type LB: lower is better, Type HB: higher is better, and Type NB: nominal is best. The combination of factor levels that yields the maximum value of the S/N ratio is the optimal condition. For the current study, fundamental frequency needs to be maximized, thus HB characteristic is to be used. Moreover, ANOVA [35] is performed to obtain the significant factors. S/N ratio analysis and ANOVA together yield the suitable setting of the design factors that optimizes the objective function. Finally, the confirmatory run verifies the optimal setting of factors obtained from the analysis.

The main advantage of the Taguchi method is that it considers a mean performance characteristic value close to the target rather than a value within specified limits. The Taguchi method is simple and easy to apply. Thus it is a powerful yet simple tool for optimization without the requirement for a large amount of experimentation. Hence it is cost-effective and less time-consuming. On the other hand, the main demerit of the method is that the results obtained are only relative and do not exactly point out which parameter has the highest effect on the performance characteristic. Moreover, since orthogonal arrays do not test all variable combinations, this method is not recommended if relationships between all variables are sought. Also, the Taguchi method fails to account for all interactions between parameters. The other demerit of the method is its offline nature. Thus it can not be applied for dynamically varying situations. Since the Taguchi approach deals with designing quality rather than correcting for poor quality, it is most effective and also recommended for early stages of process development only. Accordingly, in the present study, Taguchi methodology is applied to determine the combination of parameters that yield the maximum fundamental frequency of composite stiffened hypar shell in presence of perforations in the form of the cutout.

3. Finite Element Approach

A hypar shell with a twist radius of curvature R_{xy} is shown in Fig. 2. Here, a and b are the length and width in the plan while c is the rise of the shell, a/ and b/ are the length and width of the cutout. 1st order shear deformation theory is followed here and accordingly, the displacements are given as:

$$u = u_0(x,y) + z\theta_x(x,y)$$
$$v = v_0(x,y) + z\theta_y(x,y) \quad (1)$$
$$w = w(x,y)$$

Here u, v, and w denote the displacements in three axial (x, y, z) directions; θ_x and θ_y denote the rotations of the transverse normal about the y- and x-axes respectively. The laminated hypar shell is modeled using eight-noded isoparametric shell elements. Five degrees of freedom are considered for each node.

The element stiffness matrix is formulated using the reduced integration rule and minimum energy principle. Now, for composite materials, the constitutive matrices at the elementary level need to be obtained prior to the formulation of the stiffness matrices from the element to the global level. Here, each lamina is considered to be an orthotropic layer (Fig. 3).

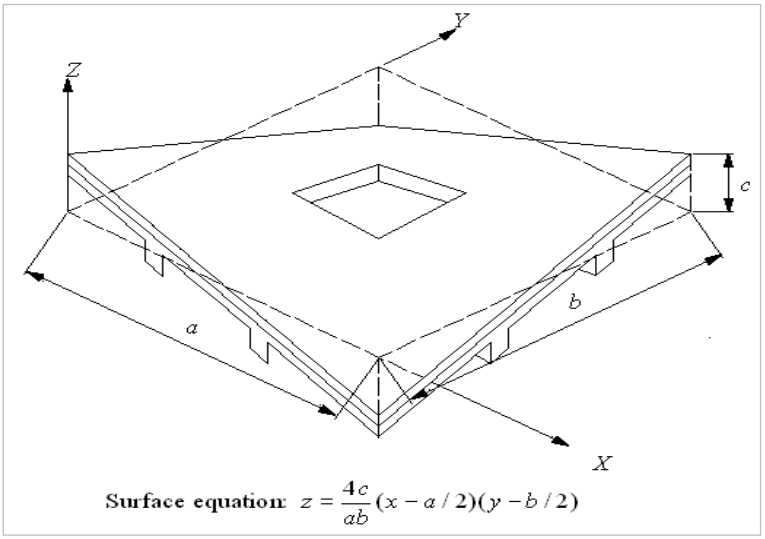

Fig. 2. Geometry of cutout borne stiffened hypar shell

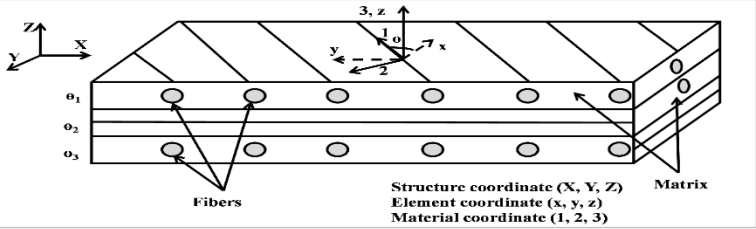

Fig. 3. Coordinate systems of laminated shell

For an element, the stress-strain relationship in the material coordinates (1, 2, 3) is written as:

$$\{\sigma'\}=[Q_1']\{\varepsilon'\};\ \{\tau'\}=[Q_2']\{\gamma'\}; \tag{2}$$

$$[Q_1']=\begin{bmatrix} \frac{E_{11}}{1-\nu_{12}\nu_{21}} & \frac{\nu_{12}E_{22}}{1-\nu_{12}\nu_{21}} & 0 \\ \frac{\nu_{21}E_{11}}{1-\nu_{12}\nu_{21}} & \frac{E_{22}}{1-\nu_{12}\nu_{21}} & 0 \\ 0 & 0 & G_{12} \end{bmatrix};$$

$$[Q_2']=\begin{bmatrix} \alpha_1 G_{13} & 0 \\ 0 & \alpha_2 G_{23} \end{bmatrix} \tag{3}$$

Here, $\{\sigma'\}$, $\{\tau'\}$, $\{\varepsilon'\}$ and $\{\gamma'\}$ are the stress and strain components (in-plane stress, shear stress, in-plane strain, and shear strain respectively) for a lamina in the material coordinates (1, 2, 3). α_1 and α_2 denote shear correction factors. E_{11} and E_{22} denote elastic moduli, while G_{12}, G_{13}, and G_{23} denote shear moduli of a lamina with respect to axes 1, 2, and 3. ν_{12}, ν_{21} denote Poisson's ratios.

The constitutive equations applicable for the lamina expressed in the element coordinates (x, y, z) are given as:

$$\{\sigma\}=[Q_1]\{\varepsilon\};\ [Q]_1=[T_1]^T[Q_1'][T_1], \tag{4}$$

$$\{\tau\}=[Q_2]\{\gamma\};\ [Q]_2=[T_2]^T[Q_2'][T_2], \tag{5}$$

$$[T_1]=\begin{bmatrix} \cos^2\theta & \sin^2\theta & \sin\theta\cos\theta \\ \sin^2\theta & \cos^2\theta & -\sin\theta\cos\theta \\ -2\sin\theta\cos\theta & 2\sin\theta\cos\theta & \cos^2\theta-\sin^2\theta \end{bmatrix}$$

$$[T_2]=\begin{bmatrix} \cos\theta & \sin\theta \\ -\sin\theta & \cos\theta \end{bmatrix} \tag{6}$$

Here, θ is taken anti-clockwise about the z-axis measuring from the x-axis to 1-axis. It may be noted here that the local coordinate system (x, y, z) for the element is a curvilinear one (Fig. 3) and is separate from the global coordinates (X, Y, Z) of the structure.

The strain-displacement relationship, constitutive equations, and formulation of stiffness and mass matrices have been provided elsewhere [25]. The modeling of the cutout with stiffeners is also presented [36, 37]. For stiffeners, the shear correction factor is usually considered as 5/6. The effect of the eccentricity of stiffeners is included by calculating the sectional parameters at the mid-surface of the shell. The connectivity matrix helps in matching the nodes of the stiffener and those of the shell. The assembly of element stiffness matrices yields the global matrices. The summation of the appropriate matrices of the shell and that of the stiffeners matched at respective nodes yield the shell mass matrix. Then assembling the element mass matrices yield the global matrices.

The position of the cutout along with its size is incorporated as input in the finite element code that generates non-uniform mesh on the shell surface. The element size is suitably controlled to decrease gradually near the cutout margins. Convergence analysis is considered for all the shell problems taken up here.

Assembly of all the mass matrices and stiffness matrices of individual elements yields a global mass matrix $[M_0]$ and global stiffness matrix $[K_0]$ respectively. The equation of motion of the shell is then written as:

$$[K_0]\{\delta\}=\omega^2[M_0]\{\delta\} \tag{7}$$

Here, ω is the natural frequency of the shell under consideration and δ is the displacement.

Now, the boundary conditions are incorporated in Eqn. (7). Then it is solved by the subspace iteration technique to obtain ω. Non-dimensional frequency is then obtained as $\overline{\omega}=\omega a^2\left(\rho/E_{22}h^2\right)^{1/2}$ where ρ is material density and h is the shell thickness.

4. Design of Experiments

DOE helps in analyzing the effect of design factors on the response characteristics. Here, the response is the fundamental frequency of the shell which is an unknown function of design factors. A large number of factors may influence the fundamental frequency. However, existing literature reveals that the fundamental frequency of laminated shells is mostly influenced by the lamination angle (A), width/thickness factor of the shell (B), and degree of orthotropy of the material (C). The shell material considered here is orthotropic and the degree of orthotropy is defined as the ratio of longitudinal to transverse Young's modulus (E_{11}/E_{22}). Thus these are

taken as design factors along with their interaction. Also, it is well documented in the literature that the position of cutout (D) influences the fundamental frequency of cutout borne shells. Thus, the position of cutout (D) is taken as the fourth design factor. Table 1 exhibits the levels of design factors within the operating range of the factors. The purpose of choosing three levels is to consider the curvature or non-linearity effects. This study is employed to consider the free vibration of laminated hypars with stiffeners and cutouts. The response variable here is the fundamental frequency. The design factors are optimized with the aim to have the maximum fundamental frequency of the shell.

According to Taguchi's philosophy, the choice of suitable OA is governed by consideration of degrees of freedom (DOFs). The DOF of chosen OA needs to be larger than or at least equal to the total DOFs needed for the analysis. In the present study, there are four design factors and each factor has three levels. For this three-level run, each main factor has (3-1) DOF. Thus, the DOF of four main factors is 4x(3-1), i.e., 8. The DOF for three two-way interactions (AxB, AxC, BxC) is 3x (3-1) x(3-1), i.e., 12. Hence, the total DOFs required for the analysis is 20. Accordingly, an L27 OA is chosen as It has 26 degrees of freedom (DOF). It contains 27 rows, each row corresponds to a test run. There are a total of 13 columns (all are not shown here in Table 2 for brevity). 1st column is alloted to lamination angle (A), 2nd column is alloted to the b/h ratio (B), the 5th column is alloted to material orthotropy (C), and the 9th column is alloted to the position of cutout (D). Six columns (3rd, 4th, 6th, 7th, 8th, 9th, and 11th) are considered for two-way interactions, and the rest three columns (10th, 12th, and 13th) are considered for error terms. The trial run is governed by the combination of the design factors and the same is shown in Table 2. It may be noted that for a full factorial design that considers four factors at three levels, the number of trial run required is 3x3x3x3 =81. On the other hand, L27 OA needs only 27 runs, i.e., a part of the full factorial design. Moreover, the array is orthogonal; and thus factor levels carry equal weights throughout the design space.

Table 1. Design factors along with level settings

Design factors	Notation in OA	Levels		
		1	2	3
Lamination angle (θ degree)	A	30	45	60
Width/thickness factor, b/h	B	20	50	100
Degree of orthotropy, E_{11}/E_{22}	C	10	25	40
Position of cutout $(\bar{x}, \bar{y})$	D	(0.2, 0.2)	(0.3, 0.3)	(0.4, 0.4)

Table 2. Experimental layout based on L27 OA

Trial No.	Lamination angle (A)	Width/thickness factor of the shell (B)	Degree of orthotropy (C)	Position of cutout (D)
1	1	1	1	1
2	1	1	2	2
3	1	1	3	3
4	1	2	1	2
5	1	2	2	3
6	1	2	3	1
7	1	3	1	3
8	1	3	2	1
9	1	3	3	2
10	2	1	1	2
11	2	1	2	3
12	2	1	3	1
13	2	2	1	3
14	2	2	2	1
15	2	2	3	2
16	2	3	1	1
17	2	3	2	2
18	2	3	3	3
19	3	1	1	3
20	3	1	2	1
21	3	1	3	2
22	3	2	1	1
23	3	2	2	2
24	3	2	3	3
25	3	3	1	2
26	3	3	2	3
27	3	3	3	1

5. Numerical Analysis

In this section, laminated stiffened hypars with the cutout are considered with eight types of end conditions, viz., SSSS, CCCC, CSCS, CSSC, FCCF, FCFC, FSFS, and FSSF. However, for brevity, the results of the SSSS boundary condition are explained in detail. The support conditions at edges are denoted by using the support as clamped support (C), simply supported (S), and free end (F) taken in an anti-clockwise order from the boundary x=0. This follows that a shell with FSFS boundary is free along the edge x=0, simply supported along the edge y=0 and free along the edge x=a and simply supported along the edge y=b. The shells are taken in square plan form (a=b) as well as the cutouts (a/=b/). The stiffeners are arranged along the cutout edge and spread up to the edge of the shell. The laminate layups of the shells are $[(\theta/-\theta)_{10}]$, i.e., a twenty-layer anti-symmetric angle ply laminate is selected for analysis. The non-dimensional coordinates of the cutout centre are denoted by ($\bar{x} = x/a, \bar{y}$= y/a,). In order to validate the stiffener formulation, the natural frequency of a centrally stiffened clamped square plate (length = width = 0.2032 m, thickness = 0.0013716 m, depth of stiffener = 0.0127 m, width of stiffener = 0.00635 m, stiffener is placed eccentric at bottom, plate material: E = 6.87x10^{10} N/m^2, ν = 0.29, ρ = 2823 kg/m^3) is obtained by the present approach. The results in Table 3 show good agreement between the present approach and with literature results [38, 39]. For validation of cutout formulation, the free vibration problem of the hypar shell with $(0/90)_4$ lamination with the cutout is taken up. Shell dimensions are taken as: a/b=1, a/h=100, a/b/=1, c/a=0.2; while material properties are chosen as: E_{11}/E_{22} = 25, G_{23} = 0.2E_{22}, G_{13} = G_{12} = 0.5E_{22}, ν_{12} =ν_{21} =0.25. Table 4 provides the fundamental frequencies of cutout borne shell and the present method compares well with literature results [40]. Thus both stiffener formulation and cutout formulation for the present code is validated with benchmark results.

Next, the fundamental frequency of stiffened hypars with the cutout is obtained as the trial run mentioned in L27 OA based on the combination of design factors. The same is then subjected to S/N ratio analysis, ANOVA analysis, and validation study. S/N ratio analysis of test data is done using Minitab [41]. As fundamental frequency needs to be maximized, the higher is better (HB) criterion of S/N ratio analysis is chosen here. S/N ratios of data (fundamental frequency) are calculated by the following relation (n is the number of observations, y_i is examined data):

$$\frac{S}{N} = -10\log\left[\frac{1}{n}\sum\left(\frac{1}{y_i^2}\right)\right] \quad (8)$$

Table 3. Fundamental frequency (Hz) of a clamped plate

Ref. [38]	Ref. [39]		Present method
	N8 (FEM)	N9 (FEM)	
711.8	725.2	725.1	733

Table 4. Fundamental frequencies ($\bar{\omega}$) of cutout borne shell

a//a	Simply supported shell		Clamped shell	
	Ref. [40]	Present model	Ref. [40]	Present model
0.0	50.829	50.825	111.600	111.612
0.1	50.769	50.779	110.166	110.233
0.2	50.434	50.400	105.464	105.443
0.3	49.165	49.178	101.350	101.490
0.4	47.244	47.141	97.987	97.991

6. Results and Discussion

Table 5 shows the fundamental frequency for the SSSS shell obtained from finite element analysis following sequential trials as per L27 OA and the corresponding S/N ratios. DOE being orthogonal, the effect of each parameter can easily be separated at different levels. Thus, the mean S/N ratio for factor A at level 1 is obtained by taking the average of S/N ratios for experiments 1-9 and so on. The mean S/N ratio for all levels of each factor A-D is presented in the response table (Table 6). The total mean of the S/N ratio is obtained as 24.08 for the SSSS shell. Table 6 also includes the delta value of every design factor. Depending on the delta value, design factors are given ranks that help to decide the impact of factors on the fundamental frequency. Table 6 shows that depending on delta value, width/thickness parameter (B) gets the rank 1, Degree of orthotropy (C) gets the rank 2, lamination angle (A) gets the rank 3 and cut-out location (D) gets the rank 4. Thus, B has the maximum influence in determining the fundamental frequency for the SSSS shell.

The main effect plot helps to observe the effect of design factors on the fundamental frequency of the concerned structure. It also identifies the optimal parametric combination that yields the maximum frequency. Figure 4 shows the main effect plot for the SSSS shell. The type of the plots explains the significance of the factors and their level of significance. If the inclination of the plot of a factor is the highest, then that factor has greater influence while the gentle slope of a factor means less influence. Figure 4 shows that the plot of factor B yields the highest inclination while that of factors C, A, and D are in decreasing order. Hence factor B is the most influencing one and other factors have little influence. It is evident from Fig. 4 that B has the highest S/N ratio at the lowest level whereas

factor C has the highest S/N ratio at its highest level, factor A contains the highest S/N ratio at the middle level, and factor D yields the highest S/N ratio value at its highest level.

Table 5. Non-dimensional fundamental frequencies and S/N ratios for SSSS shell

Trial No.	Fundamental frequency	S/N Ratio
1	18.037	25.12
2	25.804	28.23
3	31.116	29.85
4	10.211	20.18
5	14.667	23.32
6	16.453	24.32
7	8.535	18.62
8	10.624	20.52
9	14.269	23.08
10	21.563	26.67
11	30.612	29.71
12	36.373	31.21
13	11.609	21.29
14	15.778	23.96
15	19.746	25.90
16	8.35	18.43
17	12.806	22.14
18	15.747	23.94
19	18.516	25.35
20	25.184	28.02
21	31.301	29.91
22	9.74	19.77
23	14.508	23.23
24	17.858	25.03
25	8.458	18.54
26	12.157	21.69
27	12.587	21.99

The optimal parametric combination is the one where the S/N ratio achieves the maximum value. Accordingly, the optimal combination for highest fundamental frequency is A2B1C3D3, i.e., 45^0 lamination angle, width/thickness value 20, E_{11}/E_{22} ratio 40 and cut-out location (0.4, 0.4). Figure 5 represents the two-way interaction plot for SSSS shells. In an interaction graph, non-parallelism between lines means the occurrence of some level of interaction while intersecting lines indicate the occurrence of a significant interaction. In Fig. 5, non-parallel lines are obtained for (A×B) and (A×C) which implies that interaction is present for SSSS shells.

Table 6. Response table for SSSS shell

Level	A	B	C	D
1	23.7	28.23	21.56	23.71
2	24.81	23	24.54	24.21
3	23.73	21	26.14	24.32
Delta	1.11	7.23	4.59	0.61
Rank	3	1	2	4

ANOVA provides the significant design factors and interactions which mostly impact the total variance of obtained data. The results of ANOVA for SSSS shells are included in Table 7. Along with F-ratio and P-value, the ANOVA table includes the % contribution of design factors. F-ratio justifies whether a factor or interaction is significant or not. A factor having a Higher F-ratio value for a factor indicates that the factor has a higher impact. For SSSS shells, B receives the highest F-ratio value. Factors C and A follow the same.

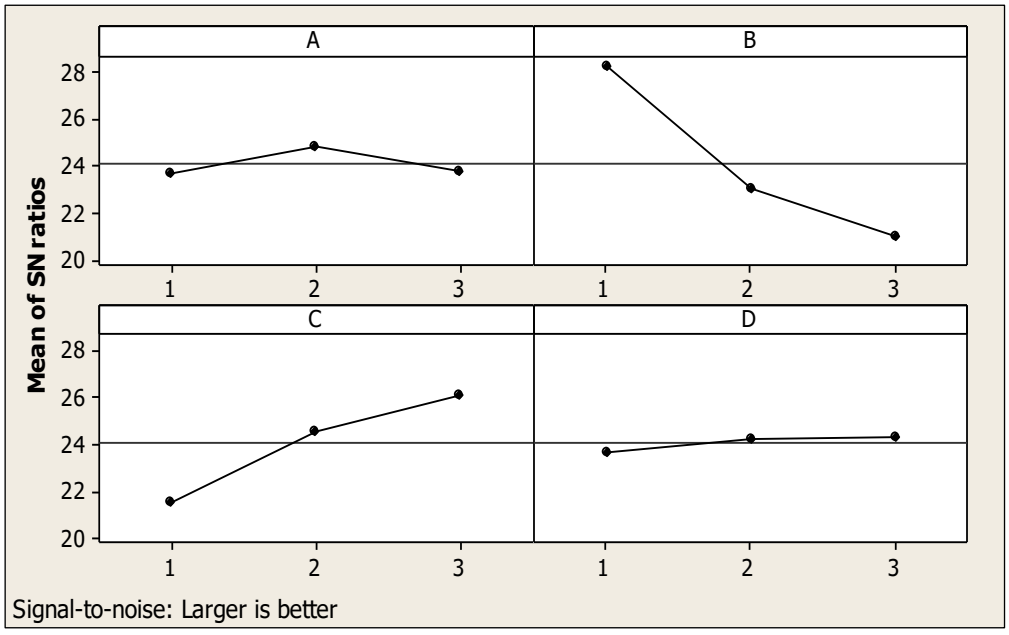

Fig. 4. Main effects plot of S/N ratios for SSSS shell

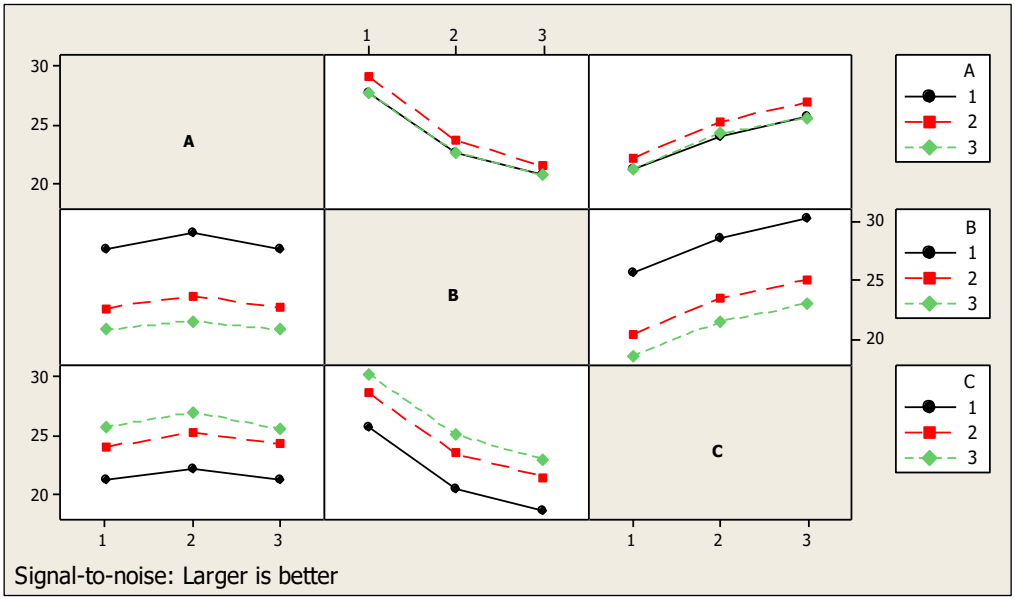

Fig. 5. Interaction plot of S/N ratios for SSSS shell

This implies that the width-to-thickness factor (B) is the most dominating factor while the degree of orthotropy (C) and lamination angle (A) have some significance. Among the interaction parameters, (A×B) and (A×C) have some significance. P-values of all the factors (except D) are below 0.005, which indicates that A, B, and C all are significant factors in controlling the fundamental frequency of SSSS shells. Table 7 also includes the percentage contribution of each factor and interaction. Here B has 69.91% contribution and C has 27.16% contribution whereas other factors and interactions contribute little.

The coefficient of determination value for the present analysis of SSSS shells is 99.87%. The normal probability plot in Fig. 6 verifies that the model is adequate. It correlates the predicted values with the data obtained from numerical analysis (finite element procedure). Figure. 6 reveals that all these data approximately lie on a straight line. Thus it establishes the adequacy of the analysis. The residual versus the fitted value of frequency is plotted in Fig. 6 and it can be seen that fitted values do not form any definite pattern, in other words, these are scattered. Thus adequacy of the model is confirmed by this. The data independency is checked by plotting residuals against test order, as included in Fig. 6. The residuals plot justified that no predictive pattern can be seen and all the residuals are scattered within allowable limits.

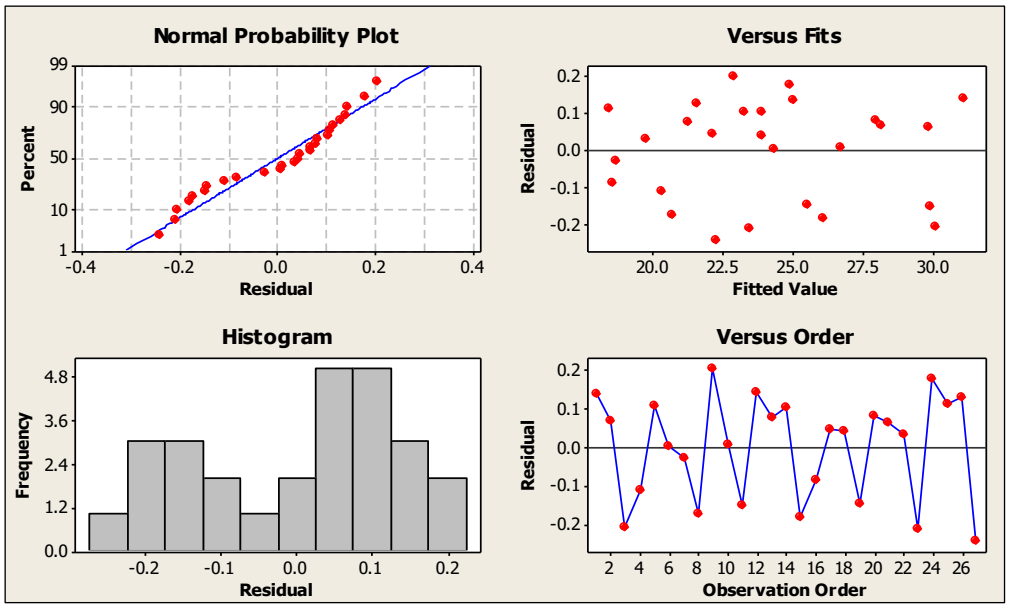

Fig. 6. Residual plots for SSSS shell

Table 7. ANOVA result for SSSS shell

Source	DF	Seq SS	Adj SS	MS	F	P	%
A	2	7.226	7.226	3.613	46.77	0	2.01
B	2	251.091	251.091	125.545	1625.25	0	69.91
C	2	97.571	97.571	48.786	631.56	0	27.16
D	2	1.908	1.908	0.954	12.35	0.007	0.53
A*B	4	0.481	0.481	0.12	1.56	0.299	0.13
A*C	4	0.353	0.353	0.088	1.14	0.42	0.09
B*C	4	0.045	0.045	0.011	0.15	0.958	0.01
Error	6	0.463	0.463	0.077			
Total	26	359.139					
S=0.277933		R-Sq=99.87%		R-Sq (adj.)=96.64%			

Lastly, a confirmatory test compares the initial factor setting with the optimal factor setting. It helps in obtaining the improvement in the final optimal result. The optimal setting of design factors is obtained using the following equation:

$$\overline{\eta} = \eta_m + \sum_{i=1}^{o} \left(\overline{\eta}_i - \eta_m\right) \tag{9}$$

Here, η_m represents the total mean of data, η_i denotes the mean of data at optimal combination, while o denotes the number of design factors with significant influence on the fundamental frequency. Table 8 provides the results of the confirmation test for SSSS shells. The S/N ratio gets improved by 7.04 dB (29.03%) compared to the initial condition. Thus, significant improvement is obtained through this procedure.

For other boundary conditions (CCCC, CSCS, CSSC, FCCF, FCFC, FSFS, and FSSF), a similar analysis is performed, however, details are omitted for brevity. Instead, salient observations are mentioned here. From ANOVA analysis results for all these boundary conditions, a summary of the contribution of the design factors on the fundamental frequency of shells is shown in Table 9. It is seen from the present study that in general with a number of boundary constraints play a pivotal role in controlling the fundamental frequency. Width/thickness factor (B) is the most dominating factor for deciding the frequency of all shell boundary conditions except CCCC shells. In the CCCC shell, the degree of orthotropy (C) is the most effective one. As the number of edge constraints is maximum in the CCCC shell, the stiffness of the shell is also maximum. So for shells with an increased number of e constraints, the rate of change of stiffness due to change in material orthotropy is higher than the rate of change of stiffness with lamination thickness. It is also found from the present study that the arrangement of boundary constraints has a significant influence on the fundamental frequency.

For CCCC shells, contributions of B and C are 39.58% and 57.45%. For CSCS shells, the same contributions are 64.81% and 28.44% while for CSSC shells these are 66.31% and 32.22% respectively.

Table 8. Confirmation table for SSSS shell

	Initial setting	Predicted setting	FE Analysis
Level	A2B2C2D2	A2B1C3D3	A2B1C3D3
Fundamental frequency	16.305		36.698
S/N ratio (dB)	24.25	29.8	31.29

Table 9. Summary of contribution (%) of design factors for different shell boundaries

Shell boundaries	Lamination angle (A)	Width/thickness factor (B)	Degree of orthotropy (C)	Position of cutout (D)
CCCC	1.29	39.58	57.45	0.21
CSCS	5.67	64.81	28.44	0.33
CSSC	0.44	66.31	32.22	0.02
SSSS	2.01	69.91	27.17	0.53
FCCF	0.13	69.41	29.81	0.11
FCFC	18.99	53.45	25.71	0.51
FSFS	0.24	77.80	21.27	0.03
FSSF	0.16	72.12	27.45	0.02

Similarly for FCCF shells, contributions of B and C are 69.41% and 29.81%; for FCFC shells, contributions of A, B and C are 18.99%, 53.45% and 25.71% respectively. For FSFS shells, contributions of B and C are 77.80% and 21.27% and for FSSF shells, these are 72.12% and 27.45% respectively. It is interesting to note here that when two opposite boundaries are clamped and the other two are free (FCFC shell), the lamination angle significantly influences the fundamental frequency. This is because, with variation in lamination angle, the direction of fiber lay changes. Accordingly, the stiffness of the shell is high when the fibers are laid in the direction of clamped edges, compared to the case when the fibers are laid in the direction of free edges. Regarding interactions, it is found from the present analysis that shells with boundary conditions like CCCC, CSCS, CSSC, FCCF, FCFC, FSFS and FSSF have interaction at (A×B) and (A×C), while FCFC shells have also some interaction at (B×C).

For different edge supports, the optimal conditions for maximum fundamental frequency are tabulated in Table 10. As already discussed earlier, the optimal condition for SSSS shells is A2B1C3D3. Similarly for shells with CCCC, CSCS, CSSC, FCCF, FCFC, FSFS and FSSF boundary conditions, the optimal predictions are A2B1C3D3, A3B1C3D2, A3B1C3D3, A1B1C3D3, A1B1C3D3, A2B1C3D1 and A3B1C3D3 respectively. Thus, it is observed that maximum fundamental frequency is obtained at the lowest level of width/thickness ratio of a shell (i.e., at b/h =20) and the highest level of degree of orthotropy (i.e., at E_{11}/E_{22} =40) for all the shell boundaries considered here.

Table 10. The optimal condition for different shell boundaries

Shell boundaries	Optimal condition
CCCC	A2B1C3D3
CSCS	A3B1C3D2
CSSC	A3B1C3D3
SSSS	A2B1C3D3
FCCF	A1B1C3D3
FCFC	A1B1C3D3
FSFS	A2B1C3D1
FSSF	A3B1C3D3

The present approach of using the Taguchi-based DOE method in the design optimization of structural response is new of its kind in the literature. Though similar methodology is well established in the process optimization of machining methods and tribology of materials [42-50]. It is believed that the present analysis will greatly help the structural engineers who design and analyze shell structures made of laminated composite materials. In the current study, the dynamic response is taken up for optimization. However, future studies may be attempted considering other structural issues like bending, buckling, post-buckling, etc. adopting a similar approach.

7. Conclusion

In this study, the fundamental frequency of cutout borne stiffened hypars made of laminated composites is obtained by numerical approach (finite element method). Taguchi technique is used for optimizing shell attributes like lamination angle, width/thickness, degree of orthotropy, and cutout location in order to have the maximum fundamental frequency. Significant shell parameters are obtained by performing an analysis of variance (ANOVA). Residual analyses testify the adequacy of the model. A confirmatory test is conducted for comparison of the initial combination with an optimal combination of factors in order to determine the improvement in the final optimal result. From this design of experiment analysis, the following conclusions are made:

1) For SSSS shell, optimum combination for highest fundamental frequency is A2B1C3D3, i.e., 45^0 lamination angle, width/thickness factor 20, E_{11}/E_{22} ratio 40 and cut-out location (0.4, 0.4).
2) Similarly for CCCC, CSCS, CSSC, FCCF, FCFC, FSFS and FSSF boundary conditions, the optimal predictions are A2B1C3D3, A3B1C3D2, A3B1C3D3, A1B1C3D3, A1B1C3D3, A2B1C3D1 and A3B1C3D3 respectively.
3) For the SSSS shell, interaction (A×B) and (A×C) have some significance. Similarly, other shells with boundary conditions like CCCC, CSCS, CSSC, FCCF, FCFC, FSFS and FSSF have interaction at (A×B) and (A×C). FCFC shell has some interaction at (B×C).
4) For different shell boundaries considered here, the width/thickness factor (B) is the most dominating factor followed by a degree of orthotropy (C). Only in the case of CCCC shells, the degree of orthotropy (C) is the most dominating factor followed by the width/thickness factor of a shell (B). Lamination angle (A) plays a significant contribution in the case of FCFC shells.
5) The position of a cutout has very little impact on all the shell boundaries considered here.
6) The maximum fundamental frequency is obtained at the lowest level of width/thickness factor (i.e., at b/h =20) and the highest level of degree of orthotropy (i.e., at E_{11}/E_{22} =40) for all the shell boundaries considered here.

Conflicts of Interest

No conflict of interest exists regarding the publication of this manuscript.

References

[1] Reddy, J.N., 1982. Large amplitude flexural vibration of layered composite plates with cutouts. *Journal of Sound and Vibration*, 83(1), pp. 1-10.

[2] Nanda, N. and Bandyopadhyay, J.N., 2007. Nonlinear free vibration analysis of laminated composite cylindrical shells with cutouts. *Journal of Reinforced Plastics and Composites*, 26(14), pp. 1413-1427.

[3] Sahoo, S., 2011. Free vibration of laminated composite hypar shell roofs with cutouts. *Advances in Acoustics and Vibrations*, 2011, pp. 1-13.

[4] Narita, Y. and Nitta, T., 1998. Optimal design by using various solutions for vibration of laminated shallow shells on shear diaphragms. *Journal of Sound and Vibration*, 214, pp. 227-244.

[5] Hufenbach, W., Holste, C. and Kroll, L., 2002. Vibration and damping behavior of multi-layered composite cylindrical shells. *Composite Structures*, 58, pp. 165-174.

[6] Narita, Y. and Robinson, P., 2006. Maximizing the fundamental frequency of laminated cylindrical panels using layerwise optimization. *International Journal of Mechanical Sciences*, 48, pp. 1516-1524.

[7] Stegmann, J. and Lund, E., 2005. Discrete material optimization of general composite shell structures. *International Journal of Numerical Methods in Engineering*, 62, pp. 2009-2027.

[8] Narita, Y., Itoh, M. and Zhao, X., 1996. Optimal design by genetic algorithm for maximum fundamental frequency of laminated shallow shells. *Advanced Composite Letters*, 5(1), pp. 21-24.

[9] Narita, Y. and Zaho, X., 1998. An optimal design for the maximum fundamental frequency of laminated shallow shells. *International Journal of Solids and Structures*, 35, pp. 2571-2583.

[10] Roy, T. and Chakraborty, D., 2009. Optimal vibration control of smart fiber reinforced composite shell structures using improved genetic algorithm. *Journal of Sound and Vibration*, 319, pp. 15-40.

[11] Topal, U., 2009. Multi-objective optimization of laminated composite cylindrical shells for maximum frequency and buckling load. *Materials & Design*, 30, pp. 2584-2594.

[12] Topal, U., 2012. Frequency optimization of laminated composite spherical shells. *Science and Engineering of Composite Materials*, 19(4), pp. 381-386.

[13] Aymerich, F. and Serra, M., 2008. Optimization of laminate stacking sequence for maximum buckling load using the ant colony optimization (ACO) metaheuristic. *Composites Part A: Applied Science and Manufacturing*, 39, pp. 262–72.

[14] Sebaey, T.A., Lopes, C.S., Blanco, N., Mayugo, J.A. and Costa, J., 2013. Two-pheromone ant colony optimization to design dispersed laminates for aeronautical structural applications. *Advances in Engineering Software*, 66(4), pp. 10–18.

[15] Erdal, O. and Sonmez, F.O., 2005. Optimum design of composite laminates for maximum buckling load capacity using simulated annealing. *Composite Structures*, 71(1), pp. 45–52.

[16] Almeida, F.S.D., 2016. Stacking sequence optimization for maximum buckling load of composite plates using harmony search algorithm. *Composite Structures*, 143, pp. 287–299.

[17] Rao, A.R.M. and Arvind, N., 2005. A scatter search algorithm for stacking sequence optimisation of laminate composites. *Composite Structures*, 70(4), pp. 383–402.

[18] Gholami, M., Fathi, A. and Baghestani, A.M., 2021. Multi-objective optimal structural design of composite superstructure using a novel MONMPSO algorithm. *International Journal of Mechanical Sciences*, 193, ID:106149.

[19] Barroso, E.S., Parente, E. and Cartaxo de Melo, A.M., 2017. A hybrid PSO-GA algorithm for optimization of laminated composites. *Structural and Multidisciplinary. Optimization*, 55(6), pp. 2111–2130.

[20] Kaveh, A., Dadras, A. and Malek, N.G., 2018. Buckling load of laminated composite plates using three variants of the biogeography-based optimization algorithm. *Acta Mechanica*, 229(4), pp. 1551–1566.

[21] Vo-Duy, T., Duong-Gia, D., Ho-Huu, V., Vu-Do, H.C. and Nguyen-Thoi, T., 2017. Multi-objective optimization of laminated composite beam structures using NSGA-II algorithm. *Composite Structures*, 168, pp. 498–509.

[22] Chaudhuri, P.B., Mitra, A. and Sahoo, S., 2022. Design of experiments analysis of fundamental frequency of laminated composite hypar shells with cut-out. *Materials Today: Proceedings*, 66 (4), pp. 2332-2337

[23] Shahgholian-Ghahfarokhi, D. and Rahimi, G., 2020. A sensitivity study of the free vibration of composite sandwich cylindrical shells with grid cores. *Iranian Journal of Science and Technology, Transactions of Mechanical Engineering*, 44, pp. 149–162.

[24] Taguchi, G., 1990. Introduction to Quality Engineering. Tokyo: Asian Productivity Organization.
[25] Sahoo, S. and Chakravorty, D., 2005. Finite element vibration characteristics of composite hypar shallow shells with various edge supports. *Journal of Vibration Control*, 11(10), pp. 1291-1309.
[26] Sahoo, S., 2015. Free vibration behavior of laminated composite stiffened elliptic parabolic shell panel with cutout. *Curved and Layered Structures,* 2(1), pp. 162-182.
[27] Duc, N.D., 2014. Nonlinear Static and Dynamic Stability of Functionally Graded Plates and Shells. Vietnam National University Press, Hanoi.
[28] Cong, P.H., Chien, T.M., Khoa, N.D. and Duc, N.D., 2018. Nonlinear thermo-mechanical buckling and post-buckling response of porous FGM plates using Reddy's HSDT. *Journal Aerospace Science and Technology*, 77, pp. 419-428.
[29] Nguyen, P.D., Papazafeiropoulos, G., Vu, Q.V. and Duc, N.D., 2022. Buckling response of laminated FG-CNT reinforced composite plates: analytical and finite element approach. *Aerospace Science and Technology*, 121, 107368.
[30] Dat, N.D., Quan, T.Q. and Duc, N.D., 2022. Vibration analysis of auxetic laminated plate with magneto-electro-elastic face sheets subjected to blast loading. *Composite Structures*, 280, 114925.
[31] Duc, N.D., Quang, V.D., Nguyen, P.D. and Chien, T.M., 2018. Nonlinear dynamic response of FGM porous plates on elastic foundation subjected to thermal and mechanical loads using the first order shear deformation theory. *Journal of Applied and Computational Mechanics*, 4(4), pp. 245-259.
[32] Duc, N.D., 2016. Nonlinear thermal dynamic analysis of eccentrically stiffened S-FGM circular cylindrical shells surrounded on elastic foundations using the Reddy's third-order shear deformation shell theory. *J. European Journal of Mechanics – A/Solids*, 58, pp.10-30.
[33] Duc, N.D., 2013. Nonlinear dynamic response of imperfect eccentrically stiffened FGM double curved shallow shells on elastic foundation. *J. Composite Structures*, 102, pp.306-314.
[34] Ross, P.J., 1996. Taguchi techniques for Quality Engineering. 2nd edn., New York: McGraw-Hill.
[35] Montgomery, D.C., 2001. Design and Analysis of Experiments. New York: Wiley.
[36] Sahoo, S. and Chakravorty, D., 2006. Stiffened composite hypar shell roofs under free vibration: behaviour and optimization aids. *Journal of Sound and Vibration*, 295, pp. 362-377.
[37] Sahoo, S., 2017. Design Aids for stiffened composite shells with cutout, Springer, Singapore.
[38] Mukherjee, A. and Mukhopadhyay, M., 1988. Finite element free vibration of eccentrically stiffened plates. *Computers and Structures*, 30, pp. 1303-1317.
[39] Nayak, A.N. and Bandyopadhyay, J.N., 2002. On the free vibration of stiffened shallow shells. *Journal of Sound and Vibration*, 255(2), pp. 357-382.
[40] Chakravorty, D., Sinha, P.K. and Bandyopadhyay, J.N., 1998. Applications of FEM on free and forced vibration of laminated shells. *ASCE Journal of Engineering Mechanics,* 124(1), pp. 1-8.
[41] Minitab User Manual (Release 13.2), 2001. Making Data Analysis Easier. MINITAB Inc., State college, PA, USA.
[42] Banerjee, S., Sutradhar, G. and Sahoo, P., 2021. Design of experiment analysis of elevated temperature wear of Mg-WC nano-composites. *Reports in Mechanical Engineering*, 2, pp. 202-211.
[43] Banerjee, S., Sarkar, P. and Sahoo, P., 2021. Improving corrosion resistance of magnesium nanocomposites by using electroless nickel coatings. *Facta Universitatis: Mechanical Engineering*, doi:10.22190/FUME210714068B.
[44] Sahoo. P., 2009. Wear behaviour of electroless Ni–P coatings and optimization of process parameters using Taguchi method. *Materials & Design*, 30(4), pp. 1341-1349.
[45] Sahoo. P., 2008. Friction performance optimization of electroless Ni–P coatings using the Taguchi method. *Journal of Physics D: Applied Physics*, 41 (9), 095305.
[46] Banerjee, S., Sahoo, P. and Davim, J.P., 2022. Tribological performance optimization of Mg-WC nanocomposites in dry sliding: A statistical approach. *Frontiers in Materials*, 9, 791447. doi: 10.3389/fmats.2022.791447.
[47] Davim, J.P. (Ed.), 2014. Modern Mechanical Engineering, Materials Forming, Machining and Tribology. Springer, Berlin, Heidelberg.
[48] Davim, J.P. (Ed.), 2012. Statistical and Computational Techniques in Manufacturing, Springer, Berlin, Heidelberg.
[49] Davim, J.P. (Ed.), 2014. Design of Experiments in Production Engineering, Management and Industrial Engineering. Springer, Cham.
[50] Davim, J.P. (Ed.), 2017. Green Composites: Materials, Manufacturing and Engineering, Berlin, Boston: De Gruyter.